EasyChair Preprint

№ 14544

Dynamic Cone Penetration in Lunar Regolith Simulant

Karlis Slumba, Brendan Scott, Mark Jaksa and Samuel Ximenes

August 26, 2024

0356 | Dynamic cone penetration in lunar regolith simulant

Kārlis Šļumba [a,*], Brendan T. Scott [a], Mark B. Jaksa [a], Samuel W. Ximenes [b]

[a] *Lunar Construction Group, Andy Thomas Centre for Space Resources, University of Adelaide, SA 5005, Australia*
[b] *Exploration Architecture Corp., San Antonio, TX 78205, United States*

** Corresponding author: karlis.slumba@adelaide.edu.au*

A B S T R A C T

Ground investigation and survey is necessary before anything can be built on the Moon. Exploration Architecture Corporation (XArc) proposed that geotechnical surveying on the Moon could be performed with a SurveyorBot; a robot equipped with cone penetrometers and seismic instruments. This research consists of development and testing of a mini dynamic cone penetrometer (Mini-DCP) with variable impact energy. The Mini-DCP will act both as a penetrometer and a seismic source, used in tandem with seismic instruments.

The purpose of this study is to investigate an appropriate range of hammering energies for a Mini-DCP to penetrate through regolith simulant. Hammering energies that are too large penetrate through the soil too fast, not providing enough data about the layering. However, hammering energies that are too low risk test stagnation and producing impact blows that may be too weak to be detected by a seismic source. This study uses bespoke Mini-DCP equipment to quantify the effects of both hammering energy and momentum. Mini-DCP test results are compared to mini cone penetration tests (Mini-CPT). Experiments are performed using engineering grade lunar highlands simulant (LHS-1E) in the regolith pit at the Extraterrestrial Environmental Simulation (EXTERRES) laboratory at the Andy Thomas Centre for Space Resources at the University of Adelaide, Australia.

Keywords
Lunar regolith
Geotechnical survey
Cone penetrometers
Soil characterization

1. Introduction

Within this decade humans will return to the Moon with National Aeronautics and Space Administration's (NASA's) Artemis program (NASA, 2020). To achieve a permanent human presence on the Moon, it is necessary to build permanent infrastructure. Before building any infrastructure projects on Earth, ground investigation and survey of the site must be performed (Rix et al., 2019), and the same will be true on the Moon. While civil engineering and construction use geotechnical data derived from well-established instruments and practices, lunar construction practices remain at low Technology Readiness Levels (TRL).

Exploration Architecture Corporation (XArc) subsidiary, Astroport Space Technologies is developing construction technologies to define a Landing/Launch Pad (LLP) construction concept of operations and a system architecture of surface assets needed for LLP site preparation and pad construction (https://explorationarchitecture.com/astroport/). Before these construction equipment assets are delivered to the lunar surface, the site needs to be surveyed for planning excavation and fill operations.

XArc is developing a lunar pathfinder called SurveyorBot under a NASA Small Business Technology Transfer (STTR) contract. The SurveyorBot will be equipped with cone penetrometers and seismic sensors to measure soil penetration resistance among other subsurface characteristics that are critical items in site leveling (Ximenes, n.d.). The idea is ultimately to deploy a swarm of semi-autonomous SurveyorBot rovers that would survey the lunar surface and immediate subsurface.

The lunar surface is covered with an unconsolidated particulate surface layer called regolith. Regolith is made by physical destruction of rock by meteorite impacts, radiation and thermal cycling called space weathering (Pieters and Noble, 2016). As opposed to the weathering processes on Earth, space weathering produces sharp particles with smaller particle sizes. A large fraction of the regolith is toxic, and electrostatically active dust adheres to all surfaces and degrades equipment (Pohlen et al., 2022). Larger meteorite impacts and landslides reveal fresh unweathered surfaces, and this process over millions of years creates a progressively deeper regolith layer. Regolith thickness can be about 10-15 m deep in lunar highlands regions, and about 4-5 m deep in mare regions (Plescia et al., 2023). Depth correlates with the age of the surface and it can differ significantly depending upon the landing site (Carrier et al., 1991). Highlands are the oldest regions of the Moon and are made from the original lunar crust. Mare regions are significantly younger and were made by volcanic eruptions of the basaltic magma, hence the regolith layer is not as thick (Heiken et al., 1991). Regolith mineralogical composition slightly differs between mare and highlands regions with mare regions being mostly basaltic (pyroxene), whereas highlands regions are mostly feldspar (Vaniman et al., 1991). Visually, highlands have higher albedo and much rougher terrain as compared to mare regions. NASA's Artemis program intends to explore the regions of the lunar south pole which are primarily made of highlands type material (Lemelin et al., 2022). Lunar highlands type material is therefore most important for this research project.

While Apollo missions returned 382 kg of lunar samples to Earth (Heiken et al., 1991), they are not accessible in large amounts. For most research projects that require testing in a lunar environment, some sort of regolith simulant is necessary. Engineering projects like this can use regolith simulants that are made for engineering purposes, and these simulants simulate

https://doi.org/10.56884/ABCD1234 *(ed. note: ISTVS will update your paper's DOI)*
ISBN 978-1-942112-57-0

geotechnical properties well, but the mineralogy is only approximate (Long-Fox et al., 2023).

Regolith is not homogeneous; it has many local layers from smaller impacts and more regional layers from large impacts. Impact debris thickness can vary substantially. From penetration and sampling experiments during Apollo, it can be seen that this heterogeneity can influence experiments. In some places, the regolith provided very little resistance to penetration (especially around crater edges), but in some places astronauts had to give up the attempts to penetrate it (especially in fresh impact ejecta) (Carrier et al., 1991). For example, penetration resistance at 40 cm depth varied between 0.3 to 1.6 MPa at Apollo 16, Station 4 and to an even higher value at Station 10.

Regolith properties might differ even further in polar regions (Sargeant et al., 2020), but the authors are not aware of a better regolith model than from the Lunar Sourcebook (Carrier et al., 1991). It has been shown that when water evaporates from regolith simulant, it can produce very loose and porous material (Šļumba et al., 2024), called a 'fairy-castle structure' (Hapke and van Horn, 1963). This is why the authors speculate that at the lunar polar region, regolith could be less compacted to deeper depths as compared to equatorial regions. This may be applicable to extinct permanently shadowed regions (PSRs) or near PSRs in the polar region or the region where the Artemis missions are aiming for.

The experiments detailed herein are performed at the Extraterrestrial Environmental Simulation (EXTERRES) laboratory at the Andy Thomas Centre for Space Resources (ATCSR) at the University of Adelaide, Australia. The EXTERRES laboratory is equipped with modern equipment (e.g. sand pit, regolith pit, vacuum chambers) to simulate the surface environment on the Moon ("Andy Thomas Centre for Space Resources | University of Adelaide," n.d.). The regolith pit is 3.1 by 3.2 m in plan dimensions and filled with 8 metric tons of engineering grade lunar highlands simulant (LHS-1E). The simulant was made by Space Resource Technologies, previously known as Exolith Lab. ("Space Resource Technologies.," n.d). The regolith simulant is on average 0.55 m deep, but the pit has some volume exclusions, so the average density can't be calculated in a straightforward manner.

2. Cone penetration tests

There are many geotechnical engineering methods for soil penetration. Some of the cone penetration methods are used in this research. The cone penetration test (CPT) consists of a cone at the end of a rod that is pushed into the soil at constant rate of 20 mm/s. By measuring the resistance of the penetration, it is possible to characterize layering and geotechnical properties of the soil. The CPT was first developed in 1932 by P. Barensten in the Netherlands (Lunne et al., 1997). The cone shape itself has not seen significant changes and the main purpose of the test remains the same. The CPT nowadays, however, can provide much more data with the additional equipment added to the test, for example, pressure, seismic, and thermal sensors (Lunne et al., 1997; White, 2022).

2.1. Dynamic cone penetration test

When comparing a dynamic cone penetrometer test (DCPT), the major difference from the CPT is that the rod is hammered into the soil instead of statically advancing it. This test is most applicable to sandy soils but is also used in silts and clays. As lunar regolith is best described as silty sand (Carrier et al., 1991), it can be expected that the DCPT will be applicable to lunar regolith. The DCPT was developed by George F. Sowers in 1959 as a simple and quick method to characterize soil compaction. The DCPT overcomes one of the most significant drawbacks of the CPT, which is the problem when encountering a stiff soil layer. For a CPT, one of the ways to penetrate through a harder layer is to increase the reaction load, but for a DCPT, this can be achieved by increasing the number of hammer drops (Sowers and Hedges, 1966).

2.2. Cone penetration on the Moon

While NASA's Apollo missions weren't the first landers on the Moon, they landed the first astronauts on 6 successful Moon landings between 1969 and 1972. The Apollo missions provided the most valuable information about the Moon to date. A detailed description of the Apollo missions and their findings is provided in the Lunar Sourcebook (Carrier et al., 1991) and references therein. Apollo 11 and 12 did not include any penetrometers, so the geotechnical properties were inferred using other indirect approaches, for example, the flagpole, core samples, digging, and photographs of the astronauts' footprints. These measurements were more qualitative in nature, but scientists were able to draw a general picture of the lunar regolith's properties. Apollo 14 incorporated a simplified cone penetrometer, and this provided better geotechnical data as compared to previous missions, but it was still very approximate. Apollo 15 and 16 had a self-recording cone penetrometer, which provided the most valuable penetration data to date.

During the Apollo missions on the Moon, astronauts encountered significant issues when trying to penetrate the lunar regolith; the biggest issue was the reduced gravity and the heterogeneous nature of the regolith layering (Carrier et al., 1991). These issues are even harder to overcome for a robotic mission, especially for a small rover. Increased penetration capability is especially important for applications on other planetary bodies like Moon and Mars where the gravity is approximately 6 and 3 times lower than on Earth respectively.

Lessons learned from the Apollo missions are the most important and most directly applicable to this research project. While Apollo missions didn't have dynamic cone penetrometers (DCPs), they still had cone penetrometers that provided useful geotechnical data and information about how the instruments operated. The Apollo findings show that the DCP would be more applicable for a geotechnical survey of the Moon, especially for a lightweight robot that can only provide a light reaction to push a penetrometer into the regolith.

The lunar regolith properties can change significantly both spatially and with depth (Plescia et al., 2023). To advance the DCP within a reasonable number of blows, an appropriate hammering energy must be quantified.

2.3. Mini dynamic cone penetrometer

Typical DCPs that are used in civil engineering, field geology and military applications are robust, large and heavy. For laboratory experiments in loose regolith simulants, the self-mass of the regular DCP is sufficient to penetrate the uncompacted soil. To tackle this issue, a mini dynamic cone penetrometer (Mini-DCP) was developed (Fig. 1). The instrument is lightweight and incorporates other parameters that can be varied. The mass of the Mini-DCP is 3 kg, excluding the mass of the hammer. This is not a flight model or a prototype, but it is made explicitly for laboratory experimentation.

Fig. 1. Mini dynamic cone penetrometer (Mini-DCP) demonstration in the sand pit, EXTERRES lab, University of Adelaide.

The Mini-DCP has an option to change the hammer mass by adding mass in increments of 500 g. The hammer can be dropped from various heights of up to a maximum of 50 cm.

The hammer impact energy comes from its potential energy E_P in Eq. 1.

$$E_P = m \cdot g \cdot h \tag{1}$$

Where m is hammer mass, g is acceleration from gravity, and h is the release height. The potential energy is transformed into kinetic energy E_K in Eq. 2.

$$E_K = \frac{1}{2} \cdot m \cdot v^2 \tag{2}$$

Where v is the impact velocity. At the time of hammer release, $E_{P,0}$ is maximum, but $E_{K,0}$ is zero, and it is opposite at the impact. As total energy of the system is constant, we can derive Eq. 3.

$$E_{P,0} + E_{K,0} = E_{P,1} + E_{K,1} \tag{3}$$

Another aspect is that it is possible to have the same energy impact with different hammer masses released at different heights. For example, hammer with mass of 0.5 kg released from 0.2 m height would have an impact energy of 0.98 J. The same energy would be produced with a 1 kg hammer that is released from a 0.1 m height.

Taking 50 mm as the minimum hammer release height, the impact energy can be varied from 0.25 to 7.5 J and momentum from 0.354 to 3.354 kg·m/s. The hammer could be dropped from a smaller height, but then the produced momentum might be too small to overcome the inertia of the Mini-DCP and to penetrate the soil. The proposed design can cover around one order of magnitude in energy and momentum levels.

The Mini-DCP cone is changeable, but for the experiments described here, the same cone from the regular DCP was used. The apex angle is 30° and the diameter of the cone is 20 mm.

3. Penetration test methodology

Filling of the regolith pit was not achieved in a controlled manner hence the density distribution is quite variable. Various individuals have been walking over the regolith simulant in recent times. The regolith simulant has been compacted by its own weight and from foot traffic, with the latter extending to a shallow depth. It was known that the simulant is not homogeneous with depth. It was hypothesized that the simulant shouldn't have much variation when comparing locations that are close to each other. Previous experiments showed that the simulant is not compacted near the edges of the regolith pit, as no one has been walking there. On the other hand, near the entrance in the pit the simulant was much more compact. The site in the central part of the pit was selected, where the conditions were expected to be similar.

A 1.2 by 1.2 m sub-section of the regolith pit was selected in the middle of the pit for experiments. As shown in Figs. 2 and 3 the sub-section was divided into 49 locations at 20 cm spacings. Based on a hypothesis that 40 by 40 cm regions should have similar conditions, locations were selected so that Mini-DCPs and Mini-CPTs would be undertaken in each region. Within each region, 9 measurements were planned, one Mini-CPT in the centre, and Mini-DCP and nuclear density gauge measurements around. As is explained below, not all nuclear density gauge measurements were able to be performed, so there were between 6 and 8 Mini-DCP measurements in each region.

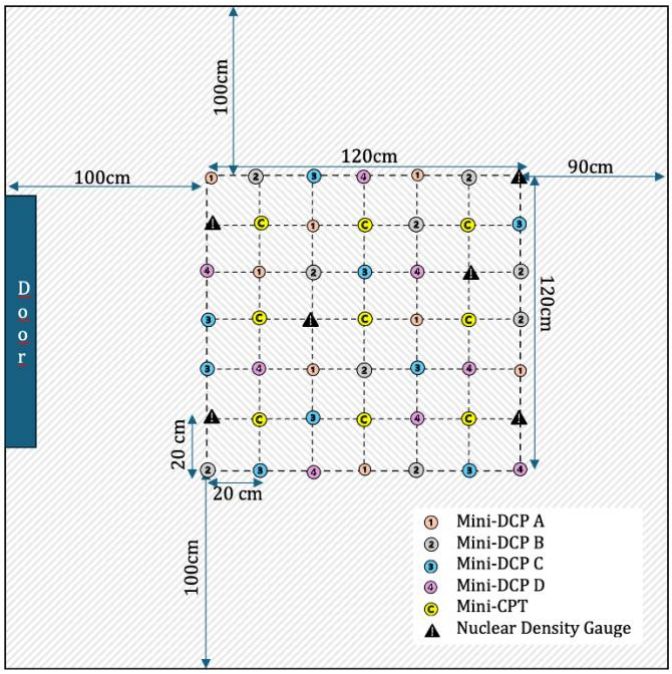

Fig. 2. Mini-DCP, Mini-CPT, and nuclear density gauge testing plan in the Regolith pit at EXTERRES lab.

Four different setups were used for the Mini-DCP, as shown in Table 1. They were scattered over the site so that each region would have at least one measurement from each setup.

Table 1. Mini-DCP setup for experiments.

Setup	Hammer mass, g	Drop height, cm	Energy, J	Momentum, kg·m/s
Mini-DCP A	477	21	0.982	0.968
Mini-DCP B	477	5	0.234	0.472
Mini-DCP C	998	10	0.978	1.397
Mini-DCP D	1497	7	1.027	1.753

The Humboldt nuclear density gauge HS-5001SD (Humboldt Nuclear Density Gauges., n.d.), normally being a very robust instrument, malfunctioned because regolith simulant found its way into the instrument and jammed the source rod mechanism. As a result, it was not possible to perform the density tests as originally intended. This highlights the important and often dismissed dust problem that exists in the lunar environment.

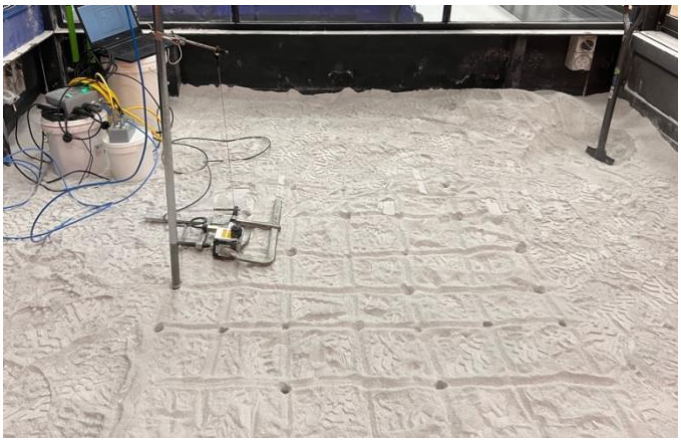

Fig. 3. Cone penetration resistance measurements in the Regolith pit at EXTERRES lab.

Mini-DCP measurements were performed using the standard DCP testing technique (Standards Australia, 1997). The number of hammer strikes required to penetrate 50 mm depth were registered. The Mini-CPT measurements were performed using a Geomil Digital CPT cone ("Geomil," n.d.). The instrument was pushed into the ground by hand, at a speed of approximately 20 mm/s.

4. Results

Mini-CPT measured penetration resistance of the regolith simulant at 9 locations in the regolith pit. Each location, together with the Mini-DCP measurements around it, accounts for a single region. Figure 4 shows a map of Pearson correlation coefficients between the penetration resistance measured by the Mini-CPT and the number of hammer strikes per 50 mm penetration. In this figure, Region 2 is identified by a red rectangle. The single blue dot in the centre is the Mini-CPT measurement for which the correlation was calculated, whereas the red dots are all Mini-DCP measurements. The highest correlations are between the measurements that are closest, meaning that the regolith structure is similar at this scale.

The Pearson correlation coefficient (r) was calculated using Eq. 4 to test the hypothesis that regions at this scale are similar, and all measurements in this region can be considered as if they sampled the same soil. Values of x and y correspond to Mini-CPT and Mini-DCP measurements at each depth, while $\bar{x}$ and $\bar{y}$ correspond to their average values.

$$r = \frac{\Sigma\big((x-\bar{x})\cdot(y-\bar{y})\big)}{\sqrt{\Sigma(x-\bar{x})^2\cdot\Sigma(y-\bar{y})^2}} \quad (4)$$

The Pearson correlation was considered high where it was higher than 0.6, average where it was between 0.4 and 0.6, and low where it was between 0.2 and 0.4. Only measurements with correlations above 0.4 were considered in the calculations.

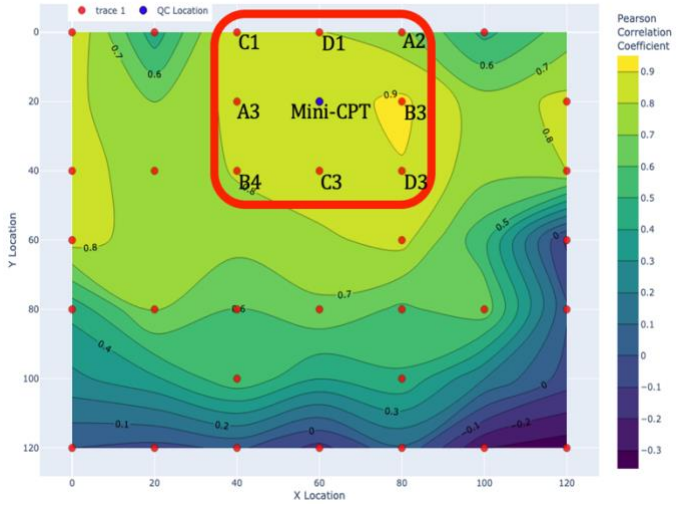

Fig. 4. Map of Pearson correlation coefficients for Mini-DCP and Mini-CPT at region 2.

A function was calculated between measurements with average and high Pearson coefficients using Eq. 5. Values of x and y correspond to Mini-CPT and Mini-DCP measurements at each depth, m is the slope and b the y-intercept.

$$y = m \cdot x + b \quad (5)$$

In this case b is set to 0, so that m becomes a multiplier or a constant by which Mini-CPT measurements should be multiplied to transform the data into units of Mini-DCP. Eq. 5 can be divided by m to arrive at Eq. 6. From this equation, m is a value by which Mini-DCP measurements should be divided to transform into units of Mini-CPT, in this case megapascal (MPa). The multiplier is in units of MPa^{-1}.

$$x = \frac{y}{m} \quad (6)$$

The multiplier m was calculated by fitting a line using least squares regression for all measurements giving 16 eligible multiplier values to transform between Mini-DCP A and Mini-CPT and 13 eligible multiplier values for each of the other Mini-DCPs. This is greater than the number of measurements because most of the Mini-DCP measurements fall into several regions. For example, Mini-DCP B4 was compared with 4 Mini-CPT measurements that are within the range.

The average multiplier values $\bar{m}$ and standard deviation σ were calculated for each setup and are shown in Table 2. One measurement of Mini-DCP B had a multiplier value that deviated from average by 3σ, this measurement was excluded from the calculations.

When all average multipliers are calculated, then all data from the Mini-DCP can be divided by the corresponding average multiplier and data in each region can be plotted on the same graph (Fig. 5). Error bars are not included on the graph because

they obscure the plot. Within the standard deviation range, all measurements yield the same result.

Table 2. Multiplier values for different Mini-DCP setups.

Setup	Measurements	$\bar{m}$, MPa^{-1}	σ, MPa^{-1}	σ, %
Mini-DCP A	16	37.8	3.5	9.2
Mini-DCP B	12	114.4	12.5	10.9
Mini-DCP C	13	24.7	4.6	18.6
Mini-DCP D	13	21.0	3.9	18.7

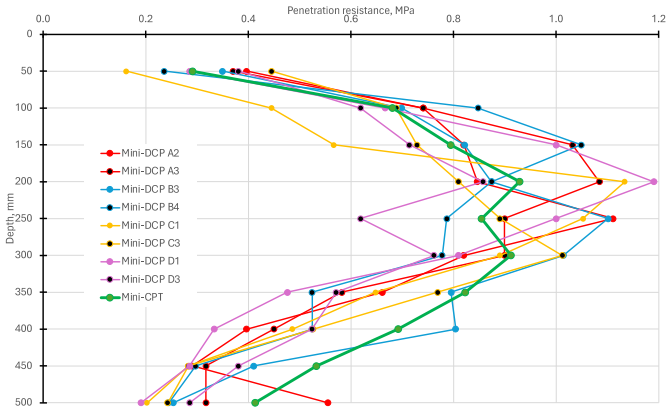

Fig. 5. Penetration resistance measured by Mini-CPT and calculated from Mini-DCP measurements.

5. Discussion

5.1. Sowers and Hedges criterion

During the preliminary experiments it was shown that the regular DCP is too heavy for this application. Sowers and Hedges (1966) explain that for the best correlation hammer drop count, there should be no fewer than 4 and no more than 30 per 4.5 cm penetration (Sowers and Hedges, 1966). With a hammer drop count that is smaller, the penetration does not provide enough data. On the other hand, where the count is too large, there is a risk of stagnation and damage to the equipment. This criterion allows to create a custom DCP that lies within this range. The previously calculated multiplier (Table 2) can be regarded as the number of hammer strikes needed to penetrate 50 mm depth at 1 MPa penetration resistance.

Penetration resistances measured during Apollo 14, 15, and 16 varies from virtually 0 to 1 MPa at 10 cm depth, from 0.3 to 1.9 MPa at 40 cm depth, and reaches more than 3 MPa at 60 cm depth. The heterogeneous regolith and variability of penetration resistance makes it difficult to determine a hammering energy that would lie within the Sowers and Hedges criterion over the entire range. Comparing the multiplier results to the Sowers and Hedges criterion, it is obvious that Mini-DCP B does not provide enough penetration at 1 MPa penetration resistance, but it would fall in the range if penetration resistance would be between 0.05 and 0.25 MPa. On the other hand, Mini-DCP D satisfies the criterion while the penetration resistance of the regolith is between 0.2 and 1.5 MPa.

5.2. Penetration in low relative density

Mini-DCP A and B setups were also tested in regolith simulant with lower relative density, where the penetration resistance is between 0.05 and 0.15 MPa. It was found that at penetration resistance below 0.12 MPa Mini-DCP sinks under its own weight. The impact of self-weight is important at low relative densities.

In this study, a multiplier was used because that is the same approach that was used by Hajduk et al. (2012). They found that sufficient correlation between DCP and CPT existed only in sand below the water table. However, they couldn't find a correlation in silt, clay or dry sand. They pointed out that one of the reasons for the large scatter in their data was the inability of DCP to detect thin layers, of which there were plenty in their soil. With the Mini-DCP, this problem is partly overcome by incorporating smaller energies.

There might be some constant values that are especially important where relative density is low, in other words, constant b in Eq. 5 might not be zero. More testing in a range of relative densities is necessary to evaluate this.

5.3. Effects of dynamic force

Loose, cohesionless soil will have smaller dynamic penetration resistance and compacted, cohesionless soil will have a larger dynamic penetration resistance as compared to a static resistance (Sowers and Hedges, 1966). This might mean that the conversion between the Mini-DCP and Mini-CPT would be linear only in a relatively narrow relative density range. More research is necessary in both lower and higher relative densities to test if this applies to regolith simulant that is not cohesionless.

Mini-DCP A, C and D all were set up to have approximately 1 J of hammer energy per strike, but different momentums, as indicated in Table 1. When comparing to the multiplier, as shown in Table 2, the multiplier decreases as the momentum increases. Testing over a larger dynamic range is necessary to find the relationship between multiplier, energy and momentum.

5.4. Boundary effects

A commonly adopted rule-of-thumb for boundary effects in penetration experiments is to keep the distance between measurements to 10 times the diameter of the penetrometer, but this can be somewhat less for loose soil. The Mini-DCP cone is 20 mm, and the Mini-CPT is 25 mm in diameter. Based on the rule-of-thumb, 200 to 250 mm distance should be necessary between measurements. The boundary effects are dependent on the internal angle of friction (ϕ) by Eq. 7 (Puech and Foray, 2002) where L is the dimension of the boundary effect, B is diameter of the cone and ϕ is the internal angle of friction.

$$L = B \cdot e^{\left(\frac{\pi}{2}\cdot\tan(\phi)\right)} \cdot \tan\left(\frac{\pi}{4}+\frac{\phi}{2}\right) \quad (7)$$

The internal angle of friction has been measured for LHS-1E to be 46° at 40% relative density and 51° at 70% relative density (Agarwal et al., 2023). Density (ρ) was measured with the nuclear density gauge to be between 1675 and 1800 kg/m^3 from the surface to 30 cm depth. Relative density (RD) was calculated using Eq. 8 where minimum (ρ_{min}) and maximum (ρ_{max}) densities of the LHS-1E are 1450 and 2000 kg/m^3 respectively (Agarwal et al., 2023).

$$RD = \frac{\rho_{max}}{\rho} \cdot \frac{\rho - \rho_{min}}{\rho_{max} - \rho_{min}} \cdot 100\% \quad (8)$$

These measurements reveal that relative density in the regolith pit was between 50 and 70%. Since the nuclear density gauge malfunctioned, additional tests were not carried out, but it is expected that relative densities as low as 40% should exist in the regolith pit. The boundary effect can be found by dividing L by B from Eq. 7. Substituting the numbers yields 12.6 for 46° and 19.6

for 51° internal angle of friction. This implies that the penetration measurements adopted in this study were too close to each other. On the other hand, the penetration holes stayed intact even when adjacent tests were performed 20 cm away; this would suggest that the influence of nearby tests was not strong enough to noticeably disturb the surface. The relative density was measured after the penetration tests were performed. This finding should be explored further and considered when planning future experiments.

5.5. Lunar analogue environment

It has been shown that the Mini-DCP can be used as a geotechnical investigation tool when operated by a human in a laboratory environment, in room temperature, and under Earth's gravity and atmosphere. However, the lunar environment provides many challenges. Laboratory experiments in a lunar analogue environment are necessary to test if this technique would work on the Moon. The regolith compaction chamber at the EXTERRES lab will allow one to simulate lunar surface properties by having a controlled density and layering of the regolith simulant. At a later stage, the Mini-DCP will be upgraded further to automatize the experiment and to make the instrument vacuum compatible. The EXTERRES lab provides a capability to use a large regolith thermal vacuum chamber, further experiments will be performed there. Simulating lunar gravity is beyond the scope of this research project, however, this experiment could be upgraded further to run it on a parabolic flight, under simulated lunar gravity.

6. Conclusions and future work

Penetration in lunar regolith simulant was measured using a Mini-DCP and a Mini-CPT. Results from both instruments were successfully correlated. A multiplier for each Mini-DCP setup was found that allows one to convert the results from one instrument to another. This research indicates that the dynamic cone penetrometer could be used to measure penetration resistance on the Moon, although more experiments are necessary to improve the reliability of this statement.

It was shown that penetration resistance of regolith simulant can be measured by a Mini-DCP. It is also possible to correlate the Mini-DCP data to other geotechnical parameters like relative density, cohesion, internal angle of friction, and compressibility.

Future work will involve equipment upgrades, for example, adding changeable cones at variety of sizes and reducing the Mini-DCP size and mass. Environmental upgrades will include controlling regolith simulant relative density from loose to dense, as well as considering layering effects. Another set of experiments will be undertaken in the regolith pit, where the Mini-DCP will be used as a seismic source.

Boundary effects depend on angle of internal friction, which is relatively high for lunar regolith simulants. It was found that spacing for penetration tests should be larger than what is typically used as a rule-of-thumb.

During this study, regolith simulant particles found their way into the instrument and jammed the source rod mechanism of the nuclear density gauge causing the equipment to malfunction. Harsh lunar environment and dangers to the equipment shouldn't be ignored.

7. Acknowledgements

This work is a part of a PhD project that is sponsored by the Andy Thomas Centre for Space Resources (ATCSR) and a University of Adelaide Research Scholarship.

Material discussed in this document is based upon work supported by NASA under contract award Number 80NSSC23PB427. Any opinions, findings, and conclusions or recommendations expressed in this material are those of the authors and do not necessarily reflect the views of the NASA.

8. Declaration of competing interest

The authors declare that they have no known competing financial interests or personal relationships that could have appeared to influence the work reported in this paper.

9. References

Agarwal, A.K., Kuo, Y.L., Jaksa, M., Scott, B., 2023. Density, strength and compressibility characteristics of lunar regolith simulant, in: Proceedings of the 14th Australia and New Zealand Conference on Geomechanics. Presented at the 14th Australia and New Zealand Conference on Geomechanics (ANZ2023), Cairns, Australia.

Andy Thomas Centre for Space Resources | University of Adelaide. n.d. EXTERRES Laboratory. https://set.adelaide.edu.au/atcsr/space-research/exterres-laboratory (accessed 24.05.24).

Carrier, W.D., III, Olhoeft, G.R., Mendell, W., 1991. Physical Properties of the Lunar Surface, in: Lunar Sourcebook, A User's Guide to the Moon. Cambridge University Press, pp. 475–594.

Geomil. n.d. Digital CPT. https://www.geomil.com/products/d-cone (accessed 24.05.24).

Hajduk, E.L., Shiver, B.T., Meng, J., 2012. A Comparison of the Sowers Dynamic Cone Penetrometer Test with Cone Penetration and Flat Blade Dilatometer Testing, in Problematic Soils and Rocks and In Situ Characterization. ASCE, pp. 1-10. https://doi.org/10.1061/40906(225)13

Hapke, B., van Horn, H., 1963. Photometric studies of complex surfaces, with applications to the Moon. Journal of Geophysical Research (1896-1977) 68, 4545–4570. https://doi.org/10.1029/JZ068i015p04545

Heiken, G., Vaniman, D., French, B.M., 1991. Lunar sourcebook: A user's guide to the Moon. Cambridge University Press.

Humboldt Nuclear Density Gauges. https://www.humboldtscientific.com/ (accessed 27.05.24).

Lemelin, M., Lucey, P.G., Camon, A., 2022. Compositional Maps of the Lunar Polar Regions Derived from the Kaguya Spectral Profiler and the Lunar Orbiter Laser Altimeter Data. Planet. Sci. J. 3, 63. https://doi.org/10.3847/PSJ/ac532c

Long-Fox, J.M., Landsman, Z.A., Easter, P.B., Millwater, C.A., Britt, D.T., 2023. Geomechanical properties of lunar regolith simulants LHS-1 and LMS-1. Advances in Space Research. https://doi.org/10.1016/j.asr.2023.02.034

Lunne, T., Robertson, P.K., Powell, J.J.M., 1997. Cone Penetration Testing In Geotechnical Practice. E&FN SPON.

NASA, 2020. NASA's Lunar Exploration Program Overview. https://www.nasa.gov/specials/artemis/

Pieters, C.M., Noble, S.K., 2016. Space weathering on airless bodies. Journal of Geophysical Research: Planets 121, 1865–1884. https://doi.org/10.1002/2016JE005128

Plescia, J.B., Cahill, J., Greenhagen, B., Hayne, P., Mahanti, P., Robinson, M.S., Spudis, P.D., Siegler, M., Stickle, A., Williams, J.P., Zanetti, M., Zellner, N., 2023. Lunar Surface Processes. Reviews in Mineralogy and Geochemistry 89, 651–690. https://doi.org/10.2138/rmg.2023.89.15

Pohlen, M., Carroll, D., Prisk, G.K., Sawyer, A.J., 2022. Overview of lunar dust toxicity risk. npj Microgravity 8, 1–9. https://doi.org/10.1038/s41526-022-00244-1

Puech, A., Foray, P., 2002. Refined Model for Interpreting Shallow Penetration CPTs in Sands. Presented at the Offshore Technology Conference, Houston, Texas. https://doi.org/10.4043/14275-MS

Rix, G.J., Wainaina, N., Ebrahimi, A., Bachus, R.C., Limas, M., 2019. Manual on Subsurface Investigations. National Academy of Sciences.

Sargeant, H.M., Bickel, V.T., Honniball, C.I., Martinez, S.N., Rogaski, A., Bell, S.K., Czaplinski, E.C., Farrant, B.E., Harrington, E.M., Tolometti, G.D., Kring, D.A., 2020. Using Boulder Tracks as a Tool to Understand the Bearing Capacity of Permanently Shadowed Regions of the Moon. Journal of Geophysical Research: Planets 125, e2019JE006157. https://doi.org/10.1029/2019JE006157

Šļumba, K., Sargeant, H.M., Britt, D.T., 2024. Development of icy regolith simulant for lunar permanently shadowed regions. Advances in Space Research 73, 3222–3234. https://doi.org/10.1016/j.asr.2024.01.014

Sowers, G.F., Hedges, C.S., 1966. Dynamic Cone for Shallow In-Situ Penetration Testing. https://doi.org/10.1520/STP44629S

Space Resource Technologies. n.d. (LHS-1E) Engineering Grade Lunar Highlands Simulant. https://spaceresourcetech.com/products/lhs-1e-simplified-lunar-highlands-simulant (accessed 24.05.2024).

Standards Australia, 1997. AS 1289.6.3.2-1997. https://www.standards.org.au/standards-catalogue/standard-details?designation=as-1289-6-3-2-1997

Vaniman, D., Dietrich, J., Taylor, G.J., Heiken, G., 1991. Exploration, Samples, and Recent Concepts of the Moon, in: Lunar Sourcebook. Cambridge University Press, pp. 5–26.

White, D.J., 2022. CPT equipment: Recent advances and future perspectives, in: Cone Penetration Testing 2022. CRC Press.

Ximenes, S. n.d. NASA SBIR STTR Contract T7.04-1837 - SurveyorBot: A Proof of Value Precursor Mission for Launch / Landing Pad Geotechnical Assessment https://sbir.nasa.gov/SBIR/abstracts/23/sttr/phase1/STTR-23-1-T7.04-1837.html (accessed 10.23.23).